

## Statistical aspects of nuclear coupling to continuum

S. Drożdż,<sup>1,2</sup> J. Okołowicz,<sup>1,2</sup> M. Płoszajczak,<sup>2</sup> and I. Rotter<sup>3</sup>

<sup>1</sup>*Institute of Nuclear Physics, Radzikowskiego 152, PL-31342 Kraków, Poland*

<sup>2</sup>*Grand Accélérateur National d'Ions Lourds, CEA/DSM-CNRS/IN2P3, BP 5027, F-14076 Caen Cedex 05, France*

<sup>3</sup>*Max-Planck-Institut für Physik Komplexer Systeme, D-01187 Dresden, Germany*

(Received 22 December 1999; published 19 July 2000)

Various global characteristics of the coupling between bound and scattering states are explicitly studied on the basis of the realistic shell model embedded in the continuum. The characteristics are related to those of the scattering ensemble. It is found that in the region of high level density, the coupling matrix elements to the continuum are consistent with the assumptions of the statistical model. However, the assumption of channel equivalence is, in general, violated and the real part of the coupling matrix elements cannot be neglected.

PACS number(s): 24.60.Ky, 21.60.Cs, 24.60.Lz

It is of great interest to relate the properties of nuclei to the ensembles of random matrices [1]. A potential agreement reflects those aspects that are generic and thus do not depend on the detailed form of the Hamiltonian matrix, while deviations identify certain system-specific, nonrandom properties of the system. On the level of bound states the related issues are quite well explored and documented in the literature [2,3]. In most cases, however, the nuclear states are embedded in the continuum and the system should be considered as an open quantum system. The applicability of the related scattering ensembles of non-Hermitian random matrices [4,5] has never been verified by an explicit calculation due to the difficulties involved in the explicit treatment of all matrix elements needed. These include a proper handling of multi-exciton internal excitations, an appropriate scattering asymptotic of the states in the continuum and a consistent and realistic coupling among them. The recently developed [6] advanced computational scheme termed the shell model embedded in the continuum (SMEC) successfully incorporates all these matrix elements. It can be used therefore to study the conditions under which the statistical description of the continuum coupling is justified.

Constructing the full SMEC solution consists of three steps. In the first step, one solves the many-body problem in the subspace  $Q$  of (quasi)bound states. For that one solves the multiconfigurational shell model (SM) problem:  $H_{QQ}\Phi_i = E_i\Phi_i$ , where  $H_{QQ} \equiv QHQ$  is the SM effective Hamiltonian which is appropriate for the SM configuration space used. For the continuum part (subspace  $P$ ), one solves the coupled channel equations:

$$(E^{(+)} - H_{PP})\xi_E^{c(+)} \equiv \sum_{c'} (E^{(+)} - H_{cc'})\xi_E^{c'(+)} = 0, \quad (1)$$

where the index  $c$  denotes different channels and  $H_{PP} \equiv PHP$ . The superscript  $(+)$  means that the boundary conditions for an incoming wave in the channel  $c$  and outgoing scattering waves in all channels are used. The channel states are defined by coupling of one nucleon in the scattering continuum to the many-body SM state in the  $(N-1)$  nucleus. Finally one solves the system of inhomogeneous coupled channel equations:

$$(E^{(+)} - H_{PP})\omega_i^{(+)} = H_{PQ}\Phi_i \equiv w_i \quad (2)$$

with the source term  $w_i$  which is primarily given by the structure of the  $N$ -particle SM wave function  $\Phi_i$ . It couples the wave functions of the  $N$ -nucleon localized states with the decay channels, i.e., with the localized states of  $(N-1)$  nucleons plus one nucleon in the continuum [6]. These equations define the functions  $\omega_i^{(+)}$ , which describe the decay of the quasibound states  $\Phi_i$  in the continuum.

The resulting full solution of the SMEC equations is then expressed as [6,7]

$$\Psi_E^c = \xi_E^c + \sum_{i,j} (\Phi_i + \omega_i) \frac{1}{E - H_{QQ}^{\text{eff}}} \langle \Phi_j | H_{QP} | \xi_E^c \rangle, \quad (3)$$

where

$$H_{QQ}^{\text{eff}} = H_{QQ} + H_{QP}G_P^{(+)}H_{PQ} \equiv H_{QQ} + W \quad (4)$$

defines the effective Hamiltonian acting in the space of quasibound states. Its first term reflects the original direct mixing of two states, while the second term originates from the mixing via the coupling to the continuum.  $G_P^{(+)}$  is the Green function for the single particle (s.p.) motion in the  $P$  subspace. The external mixing of two states, caused by  $W$ , is thus energy dependent and consists of the principal value integral and the residuum:

$$W_{ij}(E) = \sum_{c=1}^{\Lambda} \int_{\epsilon_c}^{\infty} dE' \frac{\langle \Phi_j | H_{QP} | \xi_E^c \rangle \langle \xi_E^c | H_{PQ} | \Phi_i \rangle}{E - E'} - i\pi \sum_{c=1}^{\Lambda} \langle \Phi_j | H_{QP} | \xi_E^c \rangle \langle \xi_E^c | H_{PQ} | \Phi_i \rangle. \quad (5)$$

These two terms prescribe the structure of the real  $W^R$  (Hermitian) and imaginary  $W^I$  (anti-Hermitian) parts of  $W$ , respectively. The dyadic product form of the second term allows us to express it as

$$W^I = -\frac{i}{2} \mathbf{V} \mathbf{V}^T, \quad (6)$$

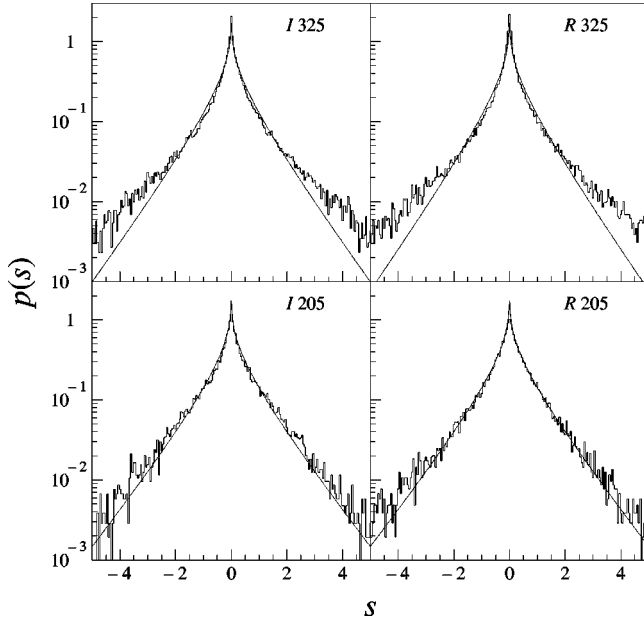


FIG. 1. Typical projections of the distribution of the matrix  $W$  elements coupling to the one channel continuum in the SM basis of  $J^\pi=0^+, T=0$  states in  $^{24}\text{Mg}$  (histograms). The projections on imaginary (left) and real axis (right) are normalized and plotted versus normalized variable  $s=(W_{ij}^X-\langle W_{ij}^X \rangle)/\sigma_X$ , where  $\sigma_X=\langle W_{ij}^X \rangle^{1/2}$ , and  $X=I,R$  denotes imaginary and real parts, respectively. In the upper parts all 325 states were taken into account, while in the lower parts only 205 states in the middle of the spectrum were included. The full curves represent  $\Lambda=1$  distribution [Eq. (7)].

where the  $M \times \Lambda$  matrix  $\mathbf{V} \equiv \{V_i^c\}$  denotes the amplitudes connecting the state  $\Phi_i (i=1, \dots, M)$  to the reaction channel  $c (c=1, \dots, \Lambda)$  [8]. This form of  $W^I$  constitutes the starting point towards a statistical description. In such a case one assumes that the internal dynamics is governed by the Gaussian orthogonal ensemble (GOE) of random matrices. This assumption can be traced to the classical chaotic scattering [9]. The orthogonal invariance arguments then imply that the amplitudes  $V_i^c$  can be assumed to be Gaussian distributed and the channels independent [4]. Assuming, as consistent with the statistical ensemble, the equivalence of the channels one then arrives at the following distribution of the off-diagonal matrix elements of  $W^I$  for  $\Lambda$  open channels:

$$\mathcal{P}_\Lambda(W_{ij}^I) = \frac{|W_{ij}^I|^{(\Lambda-1)/2} K_{(\Lambda-1)/2}(|W_{ij}^I|)}{\Gamma(\Lambda/2) \sqrt{\pi} 2^{(\Lambda-1)/2}}, \quad (7)$$

with  $\langle (W_{ij}^I)^2 \rangle = \Lambda$ .  $K_\lambda$  denotes here the modified Bessel function.

The physics to be addressed in this paper is, by making use of the above formalism, that of a nucleus decaying by the emission of one nucleon. As an example,  $^{24}\text{Mg}$  is taken with the inner core of  $^{16}\text{O}$  and the phenomenological  $sd$ -shell interaction among valence nucleons [10]. For the coupling between bound and scattering states a combination of Wigner and Bartlett forces is used, with the spin-exchange parameter  $\beta=0.05$  and the overall strength coupling  $V_{12}^{(0)}$

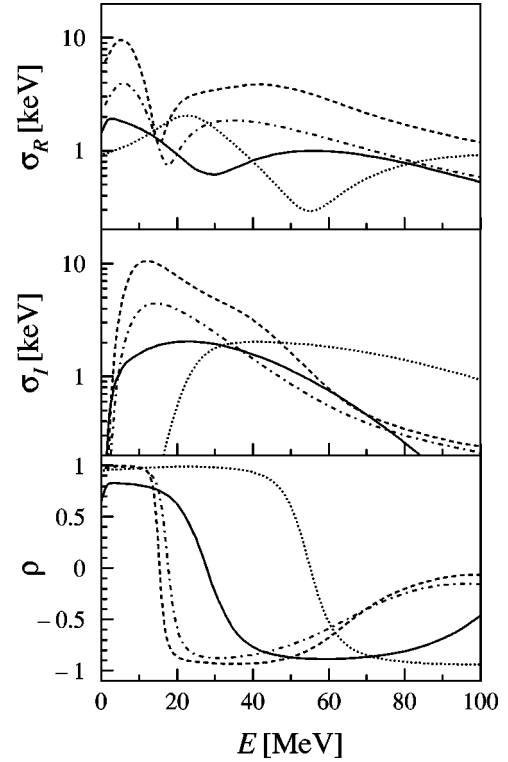


FIG. 2. Variance of real ( $\sigma_R$ ) and imaginary ( $\sigma_I$ ) parts of matrix elements  $W_{ij}$  for one open channel and correlation coefficient  $\rho = (\langle W_{ij}^R W_{ij}^I \rangle - \langle W_{ij}^R \rangle \langle W_{ij}^I \rangle) / (\sigma_R \sigma_I)$  between them. Different line styles correspond to different daughter nucleus spins: 1/2 (full line), 3/2 (dashed line), 5/2 (dot-dash), and 7/2 (dots). All these quantities are shown as a function of energy of the particle in the continuum.

$= 650 \text{ MeV fm}^3$  [6]. The radial s.p. wave functions in the  $Q$  subspace and the scattering wave functions in the  $P$  subspace are generated from the average potential of Woods-Saxon type [6].

In the above SM space, the  $^{24}\text{Mg}$  nucleus has 325  $J^\pi=0^+, T=0$  states. Depending on the particle emission threshold, these states can couple to a number of open channels. Such channels correspond to excited states in the neighboring  $N-1$  nucleus.

When testing the validity of the statistical model it is instructive to begin with one open channel and to compare the distribution of the corresponding matrix elements with formula (7) for  $\Lambda=1$ . In the example shown in Fig. 1, the open channel corresponds to spin 1/2 and its energy to about the middle of the spectrum. Both the imaginary (left) and real (right) parts of  $W$  are displayed. The upper part of Fig. 1 involves all 325  $J^\pi=0^+, T=0$  states of  $^{24}\text{Mg}$ . Clearly, there are too many large and also too many small matrix elements as compared to the statistical distribution (solid line) with  $\Lambda=1$ . This may originate from the fact that many states in the  $Q$  space are localized stronger than allowed by the GOE. It is natural to suspect that this may apply to the states close to both edges of the spectrum. Indeed, by discarding 60 states on both ends of the spectrum (205 remain), the picture changes significantly as illustrated in the lower part of Fig. 1. In this case the statistical distribution provides a good representation. Interestingly, this holds also for the real part  $W^R$

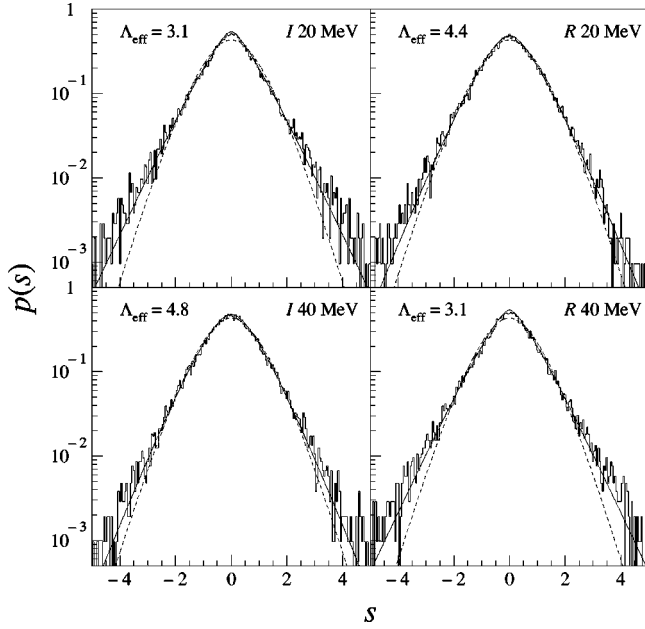


FIG. 3. The same as lower part of Fig. 1 but for ten channels of spins ranging from  $1/2$  to  $7/2$  and two energies of the particle in the continuum (depicted in the figure). The full curves represent  $\mathcal{P}_{\Lambda_{\text{eff}}}$  fits with  $\Lambda_{\text{eff}}$  indicated while the dashed curves correspond to distribution with  $\Lambda = 10$ . Only 205 states in the middle of the spectrum were included.

although the applicability of formula (7) is justified only for the imaginary part  $W^I$ . A similar behavior is found for the majority of channels, except for a small number located at the edges of the spectrum. Hence, the assumption on the Gaussian distribution of the amplitudes  $V_i^c$  is justified in a generic situation.

As for the equivalence of channels, the conditions are expected to be more intricate, especially when different channel quantum numbers are involved. The point is that the effective coupling strength depends on the quantum numbers and, in addition, on the energy  $E$  of the particle in the continuum. Thus, the proportions among the channels may vary with  $E$ . This is illustrated in Fig. 2 which shows the energy dependence of the standard deviations of the distributions (as in Fig. 1) of the relevant matrix elements for several channel spin values. Both the real and imaginary parts of  $W$  are shown, and also their correlation coefficient. Note however that within a given spin the differences are much smaller. The structures seen in Fig. 2 appear as the result of the quantum interference and are not related to the specific features of the system which is studied. Detailed investigation of these effects is beyond the scope of this paper and will be published separately.

Instead of trying to identify (with the help of Fig. 2) a sequence of  $\Lambda$  approximately equivalent channels and to verify the resulting distribution of matrix elements of  $W$  against formula (7) we find it more informative to make a random selection of such channels. An example for  $\Lambda = 10$  and two different energies ( $E = 20$  and  $40$  MeV) of the particle in the continuum is shown in Fig. 3. Among these ten randomly selected channels, two correspond to spin  $1/2$ ,

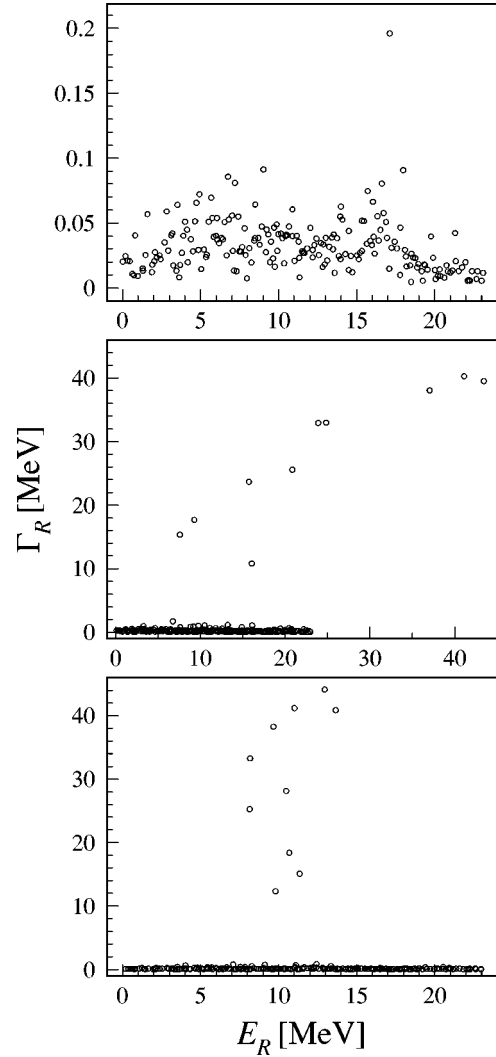


FIG. 4. 205 complex eigenvalues for ten channels and energy of the particle in the continuum of 40 MeV are presented as small circles with coordinates of  $E_R$  and  $\Gamma_R$ . The upper part represents those for the original residual interaction between  $Q$  and  $P$  subspaces. The middle one is obtained for seven times stronger interaction, and in the lower part this stronger force is applied to  $W^I$  only.

three to spin  $3/2$ , three to spin  $5/2$ , and two to spin  $7/2$ . The distributions significantly change as compared to those of the lower part of Fig. 1. Moreover,  $\mathcal{P}_{\Lambda=10}(W_{ij}^{I,R})$  [Eq. (7)] (dashed lines) does not provide an optimal representation for these explicitly calculated distributions. For  $E = 20$  MeV particle energy (the upper part of Fig. 3), the best fit in terms of the formula (7) is obtained for  $\Lambda_{\text{eff}} = 3.1$  for the imaginary part and  $\Lambda_{\text{eff}} = 4.4$  for the real part of  $W$ . At  $E = 40$  MeV one obtains  $\Lambda_{\text{eff}} = 4.8$  and  $\Lambda_{\text{eff}} = 3.1$ , correspondingly. This, first of all, indicates that effectively a smaller number of channels are involved which is caused by the broadening of the width distribution as a result of the nonequivalence of the channels [11]. Secondly, such effective characteristics depend on the energy of the particle in the continuum, which in turn is natural in view of the dependences displayed in Fig. 2. It is interesting to notice that  $W_{ij}^R$  obeys a similar distribution as

$W_{ij}^I$  although this does not result from Eq. (5) [8].

The fact that generically  $\Lambda_{\text{eff}}$  is much smaller than the actual number of open physical channels can be anticipated from their obvious nonequivalence in the majority of combinations as can be concluded from Fig. 2. The global distribution, especially in the tails, is dominated by stronger channels.

Due to the separable form of  $W$ , which in terms of  $\Lambda$  explicitly expresses its reduced dimensionality relative to  $H_{QQ}$ , an interesting related effect in the eigenvalues of  $H_{QQ}^{\text{eff}}$  may take place. For a sufficiently strong coupling to the continuum one may observe a segregation effect among the states, i.e.,  $\Lambda$  of them may separate from the remaining  $M - \Lambda$  states [12]. This effect is especially transparent when looking at the structure of  $W^I$ . For the physical strength  $V_{12}^{(0)}$  of the residual interaction in  $^{24}\text{Mg}$  this effect is negligible, as shown in the upper panel of Fig. 4. Only one state in this case separates from all others by acquiring a larger width. A magnification of the overall strength  $V_{12}^{(0)}$  of the coupling to the continuum by a constant factor  $f$  allows further states to consecutively separate. For  $f=7$ , all ten states become unambiguously separated as illustrated in the middle panel of Fig. 4. Their distance from the remaining, trapped states reflects approximately the order of their separation when  $f$  is kept increasing. This nicely illustrates the degree of nonequivalence of the channels. It further shows that  $\Lambda_{\text{eff}} \approx 5$ , being consistent with Fig. 3 at  $E=40$  MeV, is an appropriate representation for an effective number of relevant open channels. It needs to be noticed that the segregation effect takes place also in the direction of the real energy axis, though in this sense only three states uniquely separate (again consistent with  $\Lambda_{\text{eff}}=3.1$  of Fig. 3). This direction of separation originates from the real part of  $W$ . Incorporating an equivalent multiplication factor into  $W^I$  only, results in a picture as shown in the lower panel of Fig. 4. No separation in energy can be observed anymore.

In summary, the present study indicates that certain characteristics of the statistical description of the nuclear coupling to the continuum do indeed apply when the nongeneric edge effects are removed. Such a characteristic is the distribution of the coupling matrix elements to the one-channel continuum. On the other hand, the realistic SMEC calculations contain a nonequivalence of the channels which contradicts the orthogonal invariance arguments and results in a strong reduction of the number of effectively involved channels. The quantitative identification and understanding of this effect may turn out to be helpful in postulating not only improved scattering ensembles which automatically account for this effect. They may be helpful also in choosing various versions of the random matrix ensembles invented [1,13,14] in the context of bound states.

Up to now the statistical models ignore the real part of the matrix connecting the bound states to the scattering states. The real part of  $H_{QQ}^{\text{eff}}$  is likely to be dominated by  $H_{QQ}$ . Therefore, this may be not a bad approximation in some cases. Keeping in mind, however, the relatively strong energy dependence of  $W^R$  (see Fig. 2) the approximation may be worse, especially, because the segregation of states in energy (along the real axis) originates from this part. Another interesting result is that  $W^R$  is found to obey similar statistical characteristics as  $W^I$ . This does not however yet mean that the two parts of  $W$  can simply be drawn as independent ensembles. In fact, the individual matrix elements  $W_{ij}^I$  and  $W_{ij}^R$  are often strongly correlated and the degree of correlation depends on the energy of the particle in the continuum. A more detailed account of such correlations will be presented elsewhere.

We thank K. Bennaceur, E. Caurier, F. Nowacki, and M. Wójcik, for useful discussions. This work was partly supported by KBN Grant No. 2 P03B 097 16 and by Grant No. 76044 of the French-Polish Cooperation.

- 
- [1] T. A. Brody, J. Flores, J. B. French, P. A. Mello, A. Panday, and S. S. M. Wong, *Rev. Mod. Phys.* **53**, 385 (1981).
- [2] V. Zelevinsky, B. A. Brown, N. Frazier, and M. Horoi, *Phys. Rep.* **276**, 85 (1996).
- [3] S. Drożdż, S. Nishizaki, J. Speth, and M. Wójcik, *Phys. Rev. E* **57**, 4016 (1998).
- [4] V. V. Sokolov and V. G. Zelevinsky, *Nucl. Phys.* **A504**, 562 (1989).
- [5] S. Drożdż, A. Trellakis, and J. Wambach, *Phys. Rev. Lett.* **76**, 4891 (1996).
- [6] K. Bennaceur, F. Nowacki, J. Okolowicz, and M. Płoszajczak, *Nucl. Phys.* **A651**, 289 (1999); **A671**, 203 (2000).
- [7] H. W. Barz, I. Rotter, and J. Höhn, *Nucl. Phys.* **A275**, 111 (1977).
- [8] It should be noted that the real part of Eq. (6) cannot be written in the dyadic product form.
- [9] R. Blümel and U. Smilansky, *Phys. Rev. Lett.* **60**, 477 (1988); S. Drożdż, J. Okolowicz, and T. Srokowski, *Phys. Rev. E* **48**, 4851 (1993).
- [10] B. A. Brown and B. H. Wildenthal, *Annu. Rev. Nucl. Part. Sci.* **38**, 191 (1988).
- [11] E. Persson, T. Gorin, and I. Rotter, *Phys. Rev. E* **54**, 3339 (1996); **58**, 1334 (1998); see also V. A. Mandelshtam and H. S. Taylor, *J. Chem. Soc., Faraday Trans.* **93**, 847 (1997).
- [12] P. Kleinwächter and I. Rotter, *Phys. Rev. C* **32**, 1742 (1985); W. Iskra, M. Müller, and I. Rotter, *J. Phys. G* **19**, 2045 (1993); **20**, 775 (1994).
- [13] S. S. M. Wong and J. B. French, *Nucl. Phys.* **A198**, 188 (1972).
- [14] C. W. Johnson, G. F. Bertsch, and D. J. Dean, *Phys. Rev. Lett.* **80**, 2749 (1998).